

Phase equilibrium and metastability of liquid benzene at high pressures

M. Azreg-Aïnou^{a)}

Engineering Faculty, Başkent University, Bağlıca Campus, 06530 Ankara, Turkey

A. Hüseyinov

Faculty of Informatics and Management, Azerbaijan State Economic University, 370001 Baku, Azerbaijan

B. İbrahimoglu

Department of Mechanical Engineering, Gazi University, 06500 Ankara, Turkey

(Received 3 January 2006; accepted 31 March 2006; published online 24 May 2006)

This work is mainly an investigation of some of the liquid-to-solid properties of pure benzene on a restricted domain of high pressures ($20.6 \leq P \leq 102.9$ MPa). Newly obtained equilibrium experimental data and recently developed analytical equation of state are exploited and compared with each other and with previous experimental data. Curves fitted to the pressure, volume discontinuity, and enthalpy change at liquid-to-solid equilibrium points are provided. Concerning the metastable liquid benzene, both experimental and theoretical data for the minimum nucleation temperatures (limits of liquid metastability) are provided and correlated to each other. © 2006 American Institute of Physics. [DOI: 10.1063/1.2198808]

I. INTRODUCTION

Solid-liquid phase equilibrium measurements and calculations at high pressures introduce composite experimental and analytical problems.^{1–17} Solid-liquid phase transitions at high pressures have gained an increasing interest in scientific and industrial applications.^{14–21} Particularly, benzene has received broad applications in different areas of industry and the comprehensive investigations of its thermodynamic properties are rather actual problems.^{20,22}

When dealing with liquid-to-solid phase transitions another important phenomenon, from both a scientific and industrial viewpoint, occurs as the liquid is cooled below its usual transition or equilibrium temperature.^{16,23–26} Throughout this paper, the usual transition temperature is referred to as the “solidification” temperature instead of “melting” temperature.²⁷ On the other hand, the undercooling limit temperature of the liquid is referred to as the “limit of liquid metastability” or “nucleation temperature.” To our knowledge, the supercooling of liquid benzene has received very little attention with application near the triple-point temperature showing the calculated entropy changes towards two- and three-phase states that accompany the relaxation of metastable subtriple benzene.^{23,28}

In the domain of high pressures, data concerning the thermodynamic properties of liquid and solid benzene remain spread and not focused on a short range of *PVT* properties. This applies particularly to the existing pressure-temperature measurements and calculations.^{2,11,17,18,20,22} In this work we focus on the pressure range $20.6 \leq P \leq 102.9$ MPa and perform for the liquid-to-solid transition

the measurements and/or calculations of the pressures and temperatures, the molar volume discontinuities at, and enthalpy changes of solidification. Concerning the supercooled liquid benzene, we provide for $30.5 \leq P \leq 101.3$ MPa the lowest experimental nucleation temperatures that we could measure and calculate the corresponding theoretical limits of liquid metastability using a recently developed equation of state (EOS), then correlate between the sets of data.

Our measurements have been performed using the installation shown in Fig. 1 and described in Sec. II and in Refs. 29–32; very similar installations were described elsewhere.^{2,9,12,13} Our calculations are based on a recently put forward unified solid-liquid-vapor EOS.^{5,33} The developed equation writes preserving the same notations as

$$P = \frac{RT}{V - b(T)} \left(\frac{V - d}{V - c} \right) - \frac{a(T)}{V^2}, \quad (1)$$

where c and d are constants and $a(T)$ and $b(T)$ depend on the temperature through the dimensionless functions $a_r(T_r)$ and $b_r(T_r)$,

$$a = \frac{(RT_c)^2}{P_c} a_r(T_r), \quad b = \frac{Z_c RT_c}{P_c} b_r(T_r), \quad (2)$$

$$c = \frac{Z_c RT_c}{P_c} c_r, \quad d = \frac{Z_c RT_c}{P_c} d_r,$$

where the subscript c refers to the critical point, Z_c is the compressibility factor at the critical point, and the new constants c_r and d_r and the eight following constants $a_0, a_1, a_2, n, b_0, b_1, b_2,$ and m are substance dependent,

$$a_r(T_r) = a_0 + a_1 T_r \exp(-a_2 T_r^n), \quad (3)$$

^{a)}Author to whom correspondence should be addressed. Electronic mail: azreg@baskent.edu.tr

$$b_r(T_r) = b_0 + b_1 \exp(-b_2 T_r^m), \quad (4)$$

where $T_r = T/T_c$ is a reduced temperature. The corresponding numerical constants for benzene are as follows.⁵

$$\begin{aligned} P_c &= 4.894 \text{ MPa}, & T_c &= 562.05 \text{ K}, \\ Z_c &= 0.375\,029\,0, & c_r &= 0.339\,768\,6, & d_r &= 0.334\,589\,4, \end{aligned} \quad (5)$$

$$\begin{array}{l|l} a_0 = 0.311\,25, & a_1 = 1.5930 & b_0 = 0.3280, & b_1 = -9.642\,36 \times 10^{-2} \\ a_2 = 2.6678, & n = 1.51 & b_2 = 26.6560, & m = 4.0. \end{array} \quad (6)$$

The determination of the liquid-to-solid equilibrium from both Maxwell's "equal-area" Eq. (7) and Eq. (8) [derived upon rewriting and rearranging (1)] necessitates the use of a computer algebra system. For that purpose the MATLAB script M-file program is provided in the Appendix and can be translated to C or FORTRAN program.³⁴

The equal-area construction equation between the solid (V_s) and liquid (V_l) phases writes

$$\begin{aligned} P(V_l - V_s) &= RT \left[\frac{d-b}{c-b} \ln \left| \frac{V_l - b}{V_s - b} \right| + \frac{c-d}{c-b} \ln \left| \frac{V_l - c}{V_s - c} \right| \right] \\ &+ a \left(\frac{1}{V_l} - \frac{1}{V_s} \right), \end{aligned} \quad (7)$$

where P is the liquid-to-solid transition pressure and a and b are evaluated at the corresponding solidification temperature T . The molar volumes V_s and V_l , with $V_s < c < V_l$ ($c = 121.67 \text{ cm}^3$), are the real solutions of (1) at the transition pressure and temperature, which we rewrite as

$$PV^4 - AV^3 + BV^2 - CV + D = 0, \quad (8)$$

with $A = RT + (b+c)P$, $B = bcP + dRT + a$, $C = a(b+c)$, and $D = abc$.

We have performed more than 18 runs isobarically or with decreasing pressure and with a cooling rate not exceeding $0.55^\circ/\text{min}$. Only 18 runs are reported. In all cases, small perturbations in both the pressure and temperature were noticed before the freezing of the sample or during the liquid-to-solid transition. The results of our measurements and parallel evaluations are reported in the following two sections (Tables I and II).

TABLE I. Liquid-to-solid equilibrium observed data for benzene. Ten results out of the total number of runs performed are shown. Solidification pressure is in MPa and temperature in K.

P (MPa)	T (K)	P (MPa)	T (K)
20.6±1.2	284.6±0.4	67.3±1.2	297.5±0.3
31.2±1.2	287.7±0.4	77.5±1.2	300.2±0.3
41.8±1.2	291.4±0.4	87.0±1.2	303.2±0.3
53.1±1.2	294.4±0.3	98.3±1.2	305.6±0.3
58.6±1.2	295.1±0.3	102.9±1.2	306.7±0.3

II. LIQUID-TO-SOLID TRANSITION RESULTS

Figure 1 shows the installation used. The pressure in the system is set up through the dead-weight pressure gauges 1 and 17, which one pairs through the clip device 2 to the measuring vessel 4 containing the substance under consideration 12. The vessel 4 made of a stainless steel has a volume of 10 cm^3 and is located in a refrigeration cabinets 3 and 14 cooled by vapors of fluid nitrogen contained in the Dewar vessel 5. Nitrogen flows in a coil pipe of special shape that is made of a copper tube surrounding but not touching the vessel, thus ensuring a uniform cooling and even distribution of the air around the copper jacket 15. One end of the coil pipe lowers to the Dewar vessel and the other end is paired to the vacuum pump 7 through the flowmeter 8. Finally, the temperature of the substance under consideration is measured using a chromel-copel thermoelectric couple 10 of diameter of 0.2 mm paired to the electric self-recording potentiometer 9.

Table I shows the observed values of the equilibrium pressure (in megapascals) and temperature (in Kelvins) at the liquid-to-solid transition point as well as the absolute errors on the temperature and pressure. It was stated earlier that small perturbations characterized the measurements. For instance, in the temperature-time diagram the transition line was never horizontal as in theory but rather oscillated irregularly between two extreme values whose (vertical) distance is taken as the absolute error on the temperature in Table I. The liquid-to-solid transition point is identified as an average temperature of a horizontal line drawn between the two ex-

TABLE II. Liquid-to-solid and limits of liquid metastability for benzene. P_l and T_l are the transition pressure and temperature. $T_{n-\text{expt}}$ and $T_{n-\text{Theor}}$ are the experimental and theoretical limits of liquid metastability. ΔP is the pressure drop.

P_l (MPa)	T_l (K)	$T_{n-\text{expt}}$ (K)	$T_{n-\text{Theor}}$ (K)	ΔP (MPa)
30.5	288.2	270.3	255.4	3.0
40.5	290.5	273.5	257.0	2.6
50.7	293.6	277.1	259.9	2.4
54.8	294.9	278.9	261.3	2.1
60.9	296.8	281.8	263.6	1.9
71.0	299.2	284.7	266.3	1.5
80.9	301.1	287.1	268.3	1.3
101.3	306.6	294.6	278.2	0.8

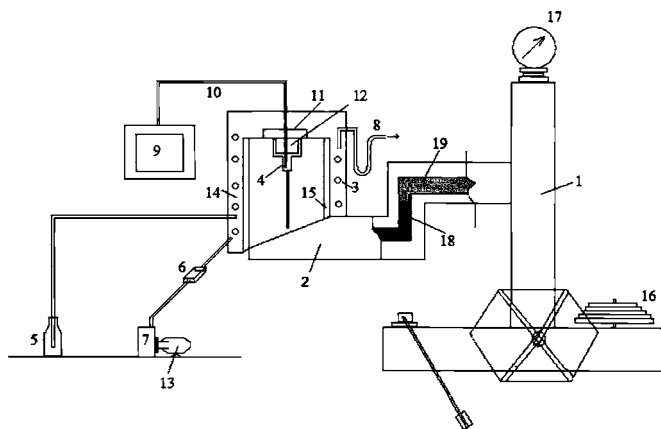


FIG. 1. Diagram of the installation used in this work. 6: regulator, 11: carving cover, 13: electric engine, 16: counterweight, 18: mercury, and 19: lubricant. The other elements are described in the text.

trime values and passing near or through the point of total solidification. The absolute error on the pressure never exceeded 1.2 MPa.

We have checked that Antoine's equation can represent with high accuracy only the upper or lower values of the data but not all the data sites shown in Table I altogether. This might be a feature of the high-pressure experiment data which sets limits to the use of Antoine's equation by contrast to the case of low-pressure and temperature data where Antoine's equation predicts with high accuracy the evaporation and sublimation curves on a wide range of temperatures.^{34,35} In order to correlate the data, we have developed and used an equation including five free parameters,³⁶

$$\log_{10} P(\text{MPa}) = A_1 - \frac{A_2}{T + A_3} - \frac{A_4}{T + A_5}; \quad (T \text{ in K}). \quad (9)$$

The advantage of Eq. (9) is that terms similar to the second (or third) one can be added, thus increasing the number of free parameters, until the desired accuracy is reached. For the set of parameters we have evaluated from the data sites,

$$\begin{aligned} A_1 &= 3.308\,29, & A_2 &= 4.996\,15, \\ A_3 &= -275.015\,91, & A_4 &= 108.407\,87, \\ A_5 &= -212.007\,545, \end{aligned} \quad (10)$$

the absolute error, $|P_{\text{data}} - P_{\text{curve}}|$, remains lower than 1.8 MPa.

Figure 2 shows the equilibrium solidification curve which is a plot of Eq. (9), our data sites shown in Table I ("o" signs), the sites whose coordinates in the PT diagram are our P data and the temperatures solutions of the system of Eqs. (7) and (8) when our P data are used as parameters ("*" signs), and the sites extracted from previous works. The upper and lower diagrams compare our work with theory and previous data, respectively.^{2,8,11} The Appendix elaborates on the resolution of Eqs. (7) and (8) with our P data used as parameters. The agreement between our equilibrium data and those obtained upon solving Eqs. (7) and (8) is fairly good. We will then rely on these equations to determine the remaining aforementioned properties.

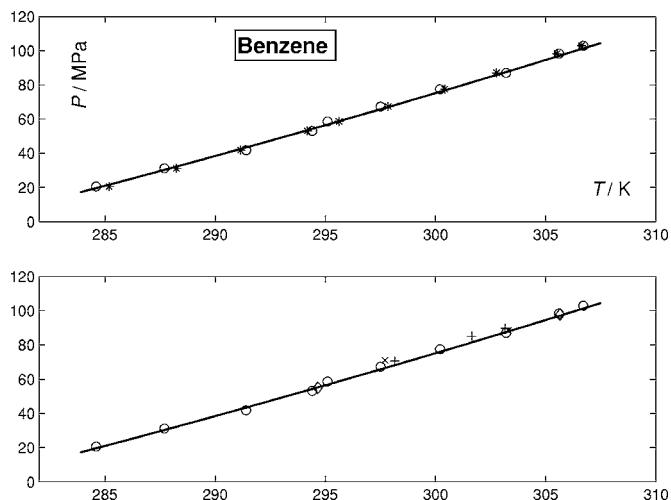


FIG. 2. PT diagram of liquid-to-solid equilibrium of benzene. Solid line: plot of the curve of Eq. (9) representing the data. The upper diagram compares our work with theory: "o" signs: data site shown in Table I, "*" signs: equilibrium data obtained upon solving Eqs. (7) and (8) with our P data used as parameters. The lower diagram compares our work with previous data: "x" signs: previous data (Ref. 11), "+" signs: previous data (Ref. 8), "◇" signs: previous data (Ref. 2).

Figure 3 shows the volume discontinuity data sites obtained upon solving Eqs. (7) and (8) (with our P data used as parameters), the line (11) fitted to the data and the data sites extracted from Ref. 8 as functions of the temperature. For the range of temperatures and pressures under consideration, the molar volume discontinuity "during solidification" is well represented by a linear function given by

$$\begin{aligned} \Delta V (\text{cm}^3 \text{mol}^{-1}) & \\ & \equiv V_l - V_s \\ & = -0.068\,936T + 29.817, \quad (T \text{ in K}). \end{aligned} \quad (11)$$

As seen from Fig. 3, most of the data extracted from (Ref. 8), which had been measured while benzene was undergoing a solid-to-liquid phase transition, are well below the line (11) fitted to our data. This could be due to the phenomenon of premelting,³⁷ which has been identified for the case of benzene at high pressures by different workers.⁶⁻⁹ Such an anomaly cannot be predicted by analytical equations (7) and (8); their resolutions provide then a "brut" volume discontinuity ΔV which is manifestly higher than that at

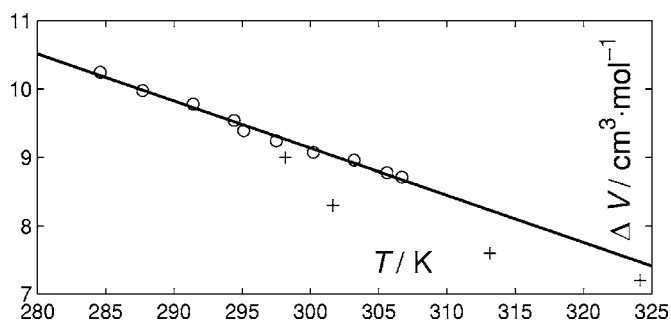


FIG. 3. Molar volume discontinuity $\Delta V \equiv V_l - V_s$ as function of temperature. "o" signs: data sites obtained upon solving Eqs. (7) and (8) with our P data used as parameters. Solid line: plot of the line of Eq. (11) fitted to the data sites. "+" signs: previous data (Ref. 8).

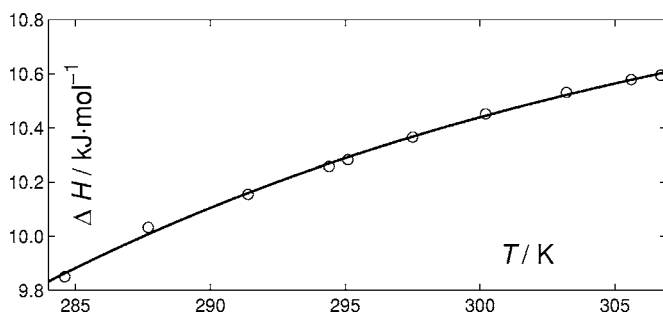


FIG. 4. Molar enthalpy change of solidification ΔH as function of temperature. “o” signs: data sites for the enthalpy change corresponding to our data shown in Table I. Solid line: plot of the cubic curve of Eq. (13) fitted to the data sites.

melt. In fact, for a normal substance undergoing premelting a thin film of liquid forms, increasing thus the molar volume of the mixture “bulk solid and thin film of liquid.” At melt, this corresponds to a lower volume discontinuity than if the substance would not undergo premelting and leads, as seen from Eq. (12), to a lowered latent heat of fusion. This latter observation was derived experimentally for the cases of Ar and Ne (Refs. 38 and 39) and obviously applies to any normal substance.

Clapeyron equation provides a way to evaluate the molar latent heat knowing the slope of the equilibrium liquid-to-solid curve and the molar volume discontinuity. The equation writes

$$\Delta H = T\Delta V(dP/dT). \quad (12)$$

Upon substituting Eqs. (9)–(11) into (12) and evaluating its right-hand side using our data (Table I), we obtained values for the enthalpy changes of solidification shown in Fig. 4 by the “o” signs. These values have an average enthalpy change of $10.31 \text{ kJ mol}^{-1}$ (Ref. 20) with a standard deviation of $0.245 \text{ kJ mol}^{-1}$ and are represented by the following cubic equation for the range of temperatures shown in Fig. 4:

$$\Delta H(\text{J mol}^{-1}) = 3.5393T^3 - 33.692T^2 + 231.94T + 10341, \quad (T \text{ in K}). \quad (13)$$

III. METASTABILITY RESULTS

The runs leading to the results shown in Table II were performed isobarically. The first and second columns of Table II show another set of observed values for the liquid-to-solid transition pressures P_t and temperatures T_t , respectively. The third column shows the minimum experimental nucleation temperatures $T_{n-\text{expt}}$ that we could reach by cooling liquid benzene before it turned to solid benzene. As the crystallization happened at $T_{n-\text{expt}}$, a drop ΔP in the gauge pressure, as shown in the fifth column, took place which was reset manually to its constant value prior to the crystallization P_t while the temperature jumped abruptly to its transition value T_t . It is straightforward to check that ΔP is directly proportional to ΔV given by (11) and that the sites ΔP vs ΔV sit randomly around, but very close to, a line with a slope of 1.76 MPa/cm^3 . The fourth column of Table II shows the results of combined numerical and theoretical

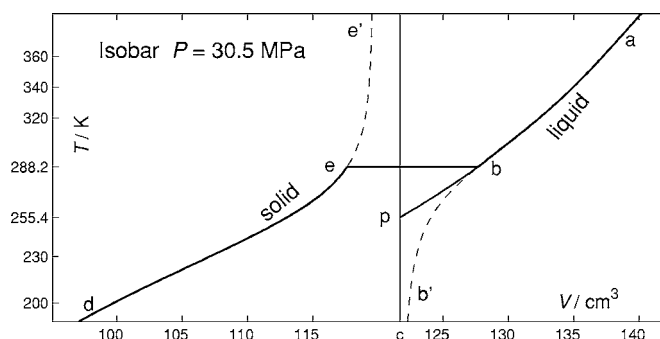


FIG. 5. A TV diagram of the isobar 30.5 MPa which is the curve $abcd$. The vertical line $V=c=121.67 \text{ cm}^3$ sets a limit between the liquid and solid regions and the horizontal line $b \rightarrow e$ is the liquid-to-solid transition line. Curve bp extends continuously and naturally the liquid properties and intersects the line $V=c$ at p where $T=T_{n-\text{theor}}=255.4 \text{ K}$, which is taken as the theoretical limit of liquid metastability. See text.

evaluations of the theoretical nucleation temperature $T_{n-\text{theor}}$ that liquid benzene can exhibit before turning to solid at the given pressure.

The theoretical limit of liquid metastability can be obtained by extending or extrapolating continuously the liquid properties to the solid region.^{40,41} In Fig. 5, the curve $abcd$ is the isobar $P=30.5 \text{ MPa}$ obtained upon plotting Eq. (1) [or (8)] in a TV diagram. The vertical line $V=c=121.67 \text{ cm}^3$ sets a limit between the liquid and solid regions and the horizontal line $b \rightarrow e$ is the theoretical liquid-to-solid transition line. The curves bb' and ee' are also plots of Eq. (1) but they are schematic, physically unrealistic extensions⁴² of the liquid and solid properties, respectively. By contrast, the line bp of cubic equation

$$T = 0.14377 \left(\frac{V - 134.41}{3.8829} \right)^3 + 2.5360 \left(\frac{V - 134.41}{3.8829} \right)^2 + 31.162 \left(\frac{V - 134.41}{3.8829} \right) + 335.42 \quad (14)$$

(T in K and V in cm^3) extends continuously and naturally the adjoining liquid curve ab by preserving the liquid properties and intersects the limiting line $V=c$ at the point p where $T=255.4 \text{ K}$, then taken as the theoretical limit temperature of liquid metastability. Another way to extend the liquid properties is to use a quadratic fitting instead of a cubic one (14), thus providing values for $T_{n-\text{theor}}$ about two degrees of temperature higher than those shown in the fourth column of Table II, which all have been obtained by a centered and scaled cubic fitting, similar to (14), of some of the sites lying on the curve ab . Hence, the values shown in the fourth column of Table II are estimate values. On the other hand, the nucleation temperatures $T_{n-\text{expt}}$ are subject to the conditions of the experimentation, which upon further improvements could lead to lower temperatures.^{43–47}

A way to correlate between the two sets of experimental and theoretical nucleation temperatures is to notice that the difference $T_t - T_n$ ($T_{n-\text{theor}}$ or $T_{n-\text{expt}}$) decreases as the pressure increases. In terms of Fig. 6, this becomes clearer if we anticipate that the slope of T_n vs T_t is slightly higher than unity, meaning that the slope of $(T_t - T_n)$ vs T_t , and consequently

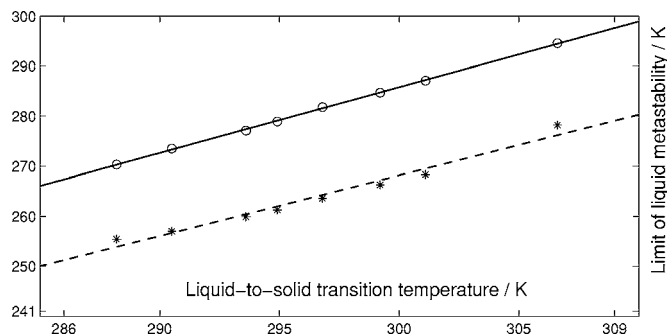


FIG. 6. A TT diagram of the experimental $T_{n-\text{expt}}$ ("o" signs) and theoretical $T_{n-\text{theor}}$ ("*" signs) limits of liquid metastability as functions of the liquid-to-solid solidification temperature T_l . The solid and dashed lines are fitted to the experimental and theoretical limits of liquid metastability data, respectively.

that of $(T_l - T_n)$ vs P_r , is negative. A further correlation between these two sets exists as explained in the Conclusion section.

IV. CONCLUSION

The derived equations (9), (11), and (13), fitted to the appropriate data, are normally valid in the range of temperatures used in this work, $284.0 \leq T \leq 307.0$ K ($20.6 \leq P \leq 102.9$ MPa). Nevertheless, Eqs. (9), (11), and (13) may remain valid beyond the assumed range of temperatures but we could not check that for all of them—lack of data for volume discontinuities and latent heats, we just verified that the transition pressure-temperature relationship (9) is applicable to the extended range of temperatures of $280.0 \leq T \leq 328.0$ K with an absolute error less than 2.4 MPa, which is lower than the discrepancy existing between some experimental data.⁸ However, this absolute error on the value of the pressure can be decreased, as we mentioned earlier, by adding a term of the form $A_6/(T+A_7)$ or more terms to Eq. (9) until the desired accuracy is reached.

It is custom to plot T_n and T_l vs P in the same diagram;²³ however, we have found it instructive to plot T_n vs T_l . Figure 6 is a temperature-temperature plot showing the experimental and theoretical limits of liquid metastability (columns 3 and 4 of Table II, respectively) versus the liquid-to-solid transition temperature. The experimental and theoretical data have been fitted to the upper and lower lines shown in Fig. 6, respectively. The correlation between the data is striking in that the lines remain almost parallel on the whole range of temperatures with a slight difference in their slopes (1.3 for the upper line and 1.2 for the lower line). The average value of the difference $T_{n-\text{expt}} - T_{n-\text{theor}}$ which is 17.25 K (with just a standard deviation of 1.28 K) may be due to impurities in the sample or microscopic crevices on the walls of the benzene container.²³ As was the case with water, we believe that a careful experiment using the technique of surfactant-stabilized emulsions^{23,43–46} or the container-less processing methods⁴⁷ will reduce the difference $T_{n-\text{expt}} - T_{n-\text{theor}}$ by providing lower values for $T_{n-\text{expt}}$.

Our anticipated conclusion is that the slope of the limit of liquid metastability versus the liquid-to-solid transition temperature will remain constant in the neighborhood of 1.3.

ACKNOWLEDGMENTS

One of us (M.A.-A.) thanks Yokozeki for sending reprints. A part of this work was carried out while one of the authors (A.H.) was at the Engineering Faculty, Başkent University.

APPENDIX: NUMERICAL RESOLUTION OF EQS. (7) AND (8)

This section provides the MATLAB codes, as a part of the numerical method, leading to the resolutions of the system of equations (7) and (8) when our P data (Table I) are used as parameters. The program is written for $P=102.9$ MPa. When the program is executed, plots of both sides of Eq. (7) as functions of the temperature are depicted showing a point of intersection. The transition temperature is the temperature of the intersection point, which is 306.62 K.

```
% A script file that calculates the 'solidification' curve
% using equations (7) and (8).
% V: molar volume in (cm3).
% T: temperature in (K).
% P: pressure in (Mpa).
% VS & VL: molar volumes of the solid & liquid at the
% transition point.
% The constants:
% Tc(K), Pc(MPa), Zc: critical temperature, critical
% pressure, critical compressibility factor.
% R(J.K-1.mol-1): the universal gas constant.
% c(cm3), d(cm3).
% Other constants: dimensionless.
% Dimensionless functions of Tr: ar, br.
% Functions of Tr: a(MPa.cm6), b(cm3).
% Application: Solid-Liquid Benzene.
clear all
cr=0.3397686; dr=0.3345894; Zc=0.3750290;
Tc=562.05; Pc=4.894; a0=0.31125; a1=1.5930;
a2=2.6678; n=1.51; b0=0.3280;
b1=-9.64236e-2; b2=26.6560; m=4.0; R=8.314510;
c=cr*(Zc*R*Tc/Pc);
d=dr*(Zc*R*Tc/Pc); vc=Zc*R*Tc/Pc; P=102.9;
syms V T VL VS;
Tr=T/Tc; ar=a0+a1*(Tr*exp(-a2*Tr^n));
br=b0+b1*exp(-b2*Tr^m);
a=((R*Tc)^2)/Pc*ar; b=(Zc*R*Tc/Pc)*br;
Ar=(d-b)/(c-b); Br=(c-d)/(c-b);
% Left-hand side of Eq. (7)
ML=P*(VL-VS);
% Right-hand side of Eq. (7)
MR=R*T*(Ar*log(abs((VL-b)/(VS-b))))...
+Br*log(abs((VL-c)/(VS-c))))...
+a*(1/VL-1/VS);
% Estimated range of the transition temperature (from
% previous data)
Td=[306.60:0.01:306.66];
A=double(subs((R*T+(b+c)*P),T,Td));
B=double(subs((b*c*P+d*R*T+a),T,Td));
C=double(subs((a*(b+c)),T,Td));
D=double(subs(a*b*c,T,Td));
```

```

% Resolution of the Eq. (8). By default, the first two
% roots are real.
% By default, the 1st root is greater than the 2nd one.
k=1;
while k <= sum(ones(size(Td)))
    s=double(solve(P*V^4-A(k)*V^3...
        +B(k)*V^2-C(k)*V+D(k)));
    Vu(k)=s(1); Vd(k)=s(2);
    k=k+1;
end
MLd=double(subs(ML,{VL,VS},{Vu,Vd}));
MRd=double(subs(MR,{VL,VS,T},{Vu,Vd,Td}));
plot(Td,MLd,'-k',Td,MRd,'-b');
xlabel ('\it T/K', 'FontSize',14)
title ('\it P=102.9 MPa', 'FontSize',16)

```

¹C. Yokoyama, T. Ebina, and S. Takahashi, *Fluid Phase Equilib.* **104**, 391 (1995).

²C. Yokoyama, T. Ebina, and S. Takahashi, *Fluid Phase Equilib.* **84**, 207 (1993).

³U. K. Deiters, *Fluid Phase Equilib.* **20**, 275 (1985).

⁴A. Yokozeki, *Appl. Energy* **81**, 322 (2005).

⁵A. Yokozeki, *Appl. Energy* **81**, 334 (2005).

⁶K. Tohji, K. Nishikawa, and Y. Murata, *Jpn. J. Appl. Phys.* **19**, L365 (1980).

⁷K. Tohji and Y. Murata, *Jpn. J. Appl. Phys., Part 1* **21**, 1199 (1982).

⁸P. Figuière, A. H. Fuchs, M. Ghelfenstein, and H. J. Szwarc, *J. Phys. Chem. Solids* **39**, 19 (1978).

⁹A. H. Fuchs, Ph. Pruzan, and L. Ter Minassian, *J. Phys. Chem. Solids* **40**, 369 (1979).

¹⁰I. Czarnota, *J. Chem. Thermodyn.* **23**, 25 (1991).

¹¹N. Nagaoka and T. Makita, *Int. J. Thermophys.* **8**, 415 (1987).

¹²Ph. Pruzan, L. Ter Minassian, P. Figuière, and H. Szwarc, *Rev. Sci. Instrum.* **47**, 66 (1976).

¹³L. Ter Minassian and Ph. Pruzan, *J. Chem. Thermodyn.* **9**, 375 (1977).

¹⁴D. A. Kofke, *J. Chem. Phys.* **98**, 4149 (1993).

¹⁵D. M. Heyes, *The Liquid State: Applications of Molecular Simulations* (Wiley, Chichester, 1998).

¹⁶B. Vinet, L. Magnusson, H. Fredriksson, and P. J. Desré, *J. Colloid Sci.* **255**, 363 (2002).

¹⁷J. Akella and G. C. Kennedy, *J. Chem. Phys.* **55**, 793 (1971).

¹⁸*Handbook of Physical Quantities*, edited by I. S. Grigoriev and G. C. Kennedy (CRC, Boca Raton, Florida, 1997).

¹⁹*American Institute of Physics Handbook*, 3rd ed., edited by D. E. Gray (McGraw-Hill, New York, 1972).

²⁰National Institute of Standards and Technology, <http://webbook.nist.gov/chemistry/>

²¹*Encyclopedia of Chemical Physics and Physical Chemistry*, edited by J. H. Moore and N. D. Spencer (Institute of Physics, Bristol, 2001).

²²L. Ciabini, F. A. Gorelli, M. Santoro, R. Bini, V. Schettino, and M. Mezouar, *Phys. Rev. B* **72**, 094108-1 (2005).

²³P. G. Debenedetti, *Metastable Liquids: Concepts and Principles* (Princeton University Press, Princeton, NJ, 1996).

²⁴*Crystal Growth and Materials*, edited by E. Kaldis and H. J. Scheel (North-Holland, Amsterdam, 1977).

²⁵*Crystal Growth of Electronic Materials*, edited by E. Kaldis (North-Holland, Amsterdam, 1985).

²⁶B. İbrahimoglu, A. F. Guseynov, and R. Alibeyli, Contribution to the Ninth International Conference on Hydrogen Materials Science and Chemistry of Carbon Nanomaterials, Sevastopol, Ukraine, September 2005 (unpublished).

²⁷At high pressures, the transition from solid to liquid of benzene is not abrupt, rather anticipated by a premelting phase. Such an anomaly makes the determination of the melting temperature rather difficult.

²⁸M. C. D'Antonio, Ph.D. thesis, Princeton University Princeton, NJ, 1989.

²⁹B. İbrahimoglu and A. M. Rehimov, *Phase Transitions in Liquids* (Azerbaijan Academy of Science, Baku, 1984), pp. 1-12.

³⁰B. İbrahimoglu and A. M. Rehimov, *Engineering Physics Review* **19**, 498 (1985).

³¹B. İbrahimoglu, Y. M. Naziyev, and N. F. Aliyev, Contribution to the Scientific and Technical Congress on Heat Processes, Baku, Azerbaijan, 1992 (unpublished).

³²B. İbrahimoglu and N. F. Aliyev, Contribution to the Scientific and Technical Congress on Heat Processes, Baku, Azerbaijan, 1986 (unpublished).

³³A. Yokozeki, *Int. J. Thermophys.* **24**, 589 (2003).

³⁴Mj. Assael, J. P. M. Trusler, and T. F. Tsolakis, *Thermophysical Properties of Fluids* (Imperial College Press, London, 1996).

³⁵M. Azreg-Aïnou, *Monatsch. Chem.* **136**, 2017 (2005).

³⁶M. Azreg-Aïnou, Contribution to the Eighth International Conference on Carbon Dioxide Utilization, Oslo, Norway, June 2005 (unpublished).

³⁷J. G. Dash, H. Fu, and J. S. Wettlaufer, *Rep. Prog. Phys.* **58**, 115 (1995).

³⁸D. M. Zhu and J. G. Dash, *Phys. Rev. Lett.* **57**, 2959 (1986).

³⁹D. M. Zhu and J. G. Dash, *Phys. Rev. Lett.* **60**, 432 (1988).

⁴⁰J. Kestin, *A Course in Thermodynamics* (Hemisphere, New York, 1979).

⁴¹M. D. Ediger, C. A. Angell, and S. R. Nagel, *J. Phys. Chem.* **100**, 13200 (1996).

⁴²In a more realistic model, the isobars should have a minimum value in the liquid region and a maximum value in the solid region whose temperatures are the limits of metastability.

⁴³D. H. Rasmussen and A. P. Mackenzie, *J. Chem. Phys.* **59**, 1003 (1973).

⁴⁴D. H. Rasmussen, A. P. Mackenzie, C. A. Angell, and J. C. Tucker, *Science* **181**, 342 (1973).

⁴⁵H. Kanno, R. J. Speedy, and C. A. Angell, *Science* **189**, 881 (1975).

⁴⁶C. A. Angell and H. Kanno, *Science* **193**, 1121 (1976).

⁴⁷D. W. Gomersall, S. Y. Shiraishi, and R. G. Ward, *J. Aust. Inst. Met.* **10**, 220 (1965).